

Stress Analysis of Steam-Methane Reformer Tubes

by

Khairul Anwar Bin Hasni

Dissertation submitted in partial fulfilment of
the requirements for the
Bachelor of Engineering (Hons)
(Mechanical Engineering)

MAY 2012

Universiti Teknologi PETRONAS,
Bandar Seri Iskandar,
31750, Tronoh,
Perak Darul Ridzuan.

CERTIFICATION OF APPROVAL

Stress Analysis of Steam-Methane Reformer Tubes

by

Khairul Anwar Bin Hasni

A project dissertation submitted to the
Mechanical Engineering Programme
Universiti Teknologi PETRONAS
In partial fulfilment of the requirement for the
BACHELOR OF ENGINEERING (Hons)
(MECHANICAL ENGINEERING)

Approved by,

(Dr. Azmi bin Abdul Wahab)

UNIVERSITI TEKNOLOGI PETRONAS
TRONOH, PERAK
MAY 2012

CERTIFICATION OF ORIGINALITY

This is to certify that I am responsible for the work submitted in this project, that the original work is my own except as specified in the references and acknowledgements, and that the original work contained herein have not been undertaken or done by unspecified sources or persons.

KHAIRUL ANWAR BIN HASNI

ABSTRACT

A steam-methane reformer (SMR) tube is very important in oil refinery industry. An SMR tube is a device used in steam reforming or auto thermal reforming, and it is a type of chemical synthesis which can produce pure hydrogen gas from natural gas using a catalyst. The tube is expected to last 100,000 hours or 11.4 years but in many instances some of these tubes fail prematurely. Since the material cost is a large investment, thorough analyses are necessary to predict possible failure of the steam reformer tube in order to save operation and downtime cost. In order to reliably predict the performance of the tube, good assessment of the stresses acting at any point along the tube length and thickness is needed.

In this project, Finite Element Method (FEM) was used to perform the stress analysis of the tube and the analysis considered the disparity in stresses along the tube length and thickness due to temperature and pressure differences. ANSYS software was used in performing the analysis. Both 2D axisymmetric and 3D approach were used in the analyses. The 2D axisymmetric models represent a slice of the actual 3D model that, if revolved around the y-axis of the reference Cartesian coordinate system, would become the original 3D structure. The advantage of using a 2D axisymmetric model compared to a 3D model is the reduced in calculation time and it is easier to change details to the geometry. Two types of analyses were performed, stress analysis due to internal pressure and stress analysis due to difference in temperature along the tube. In the first analysis, the von Mises stress was highest at the inner wall of the tube and lowest at the center of the tube wall. For the second analysis, it was shown that the von Mises stress decreased from inner wall to minimum near the center of the tube wall and then increased to the outer tube wall.

TABLE OF CONTENTS

CERTIFICATION OF APPROVAL	i
CERTIFICATION OF ORIGINALITY	ii
ABSTRACT	iii
TABLE OF CONTENTS	iv
LIST OF FIGURES	v
LIST OF TABLES	vii
CHAPTER 1 : INTRODUCTION	1
1.1 Background of Study	1
1.2 Problem Statement	2
1.3 Objective and Scope of Study	2
CHAPTER 2 : LITERATURE REVIEW	4
2.1 Steam-Methane Reforming (SMR) Process	4
2.2 Analytical Equations	6
CHAPTER 3 : METHODOLOGY	8
3.1 Finite Element Analysis	8
3.2 SMR ANSYS Workflow	9
3.3 Gantt Chart	11
CHAPTER 4 : RESULTS AND DISCUSSION	13
4.1 Parameters of Stress Analysis of Steam-Methane Reformer Tubes.....	13
4.2 Analysis of Internal Pressure on SMR Tube Wall	14
CHAPTER 5 : CONCLUSION AND RECOMMENDATION	34
REFERENCE.....	36

LIST OF FIGURES

Figure 1.1: General view of SMR tubes	3
Figure 2.1 : Schematic process of Steam Methane Reformer[3].	4
Figure 2.2 : SMR in operation[4].....	5
Figure 2.3 : Inside view of the SMR[5].	5
Figure 3.1 : ANSYS learning flowchart.....	9
Figure 3.2 : Material model behavior box.....	9
Figure 3.3 : Boundary condition and pressure applied at SMR tube wall.	10
Figure 3.4 : Stress stress occurred at the tube after the problem was solved.	11
Figure 3.5: Gantt Chart for Final Year Project 2.	12
Figure 4.1 : von Mises stress of 2D axisymmetric's internal pressure simulation of SMR tube for N1 parameters.	15
Figure 4.2 : von Mises stress of 3D ANSYS simulation due to internal pressure of SMR tube for N1 parameters.	17
Figure 4.3 : Comparison of line trend between 2D ANSYS, 3D ANSYS and analytical calculation of effective stress due to internal pressure for N1.	20
Figure 4.4 : Analytical effective stress due to internal pressure versus tube radius. .	21
Figure 4.5 : Effective stress of 2D ANSYS analysis due to internal pressure versus tube radius.	21
Figure 4.6 : Effective stress of 3D ANSYS analysis due to internal pressure versus tube radius.	22
Figure 4.7 : Overlapping of analytical, 2D and 3D pressure analysis.....	22
Figure 4.8 : 3D thermal ANSYS analysis modelling for N1 parameters.....	24
Figure 4.9 : Comparison of line trend between 3D thermal ANSYS analysis and analytical calculation of effective stress due to temperature for sample N1.....	26
Figure 4.10 : Analytical effective stress due to temperature distribution versus tube radius.	27
Figure 4.11 : 3D ANSYS analysis effective stress due to temperature distribution versus tube radius.....	27
Figure 4.12 : 3D thermal and internal pressure ANSYS analysis modelling of quarter SMR tube.	29

Figure 4.13 : Comparison of line trend between 3D ANSYS analysis and analytical calculation of effective stress due to temperature and internal pressure for sample N1.	32
Figure 4.14 : Theoretical effective stress due to temperature and pressure versus tube radius.	33
Figure 4.15 : ANSYS analysis effective stress due to temperature and pressure versus tube radius.	33
Figure 5.1 : 3D images of creep failure on SMR tube by LOTIS system[9].	35

LIST OF TABLES

Table 4.1: Input parameters for finite element analysis.....	13
Table 4.2 : Analytical results of internal pressure analysis.....	14
Table 4.3 : Stress comparison due to internal pressure between analytical calculations and 2D ANSYS analysis.	15
Table 4.4 : Internal pressure 2D ANSYS analysis results.	16
Table 4.5 : Effective stress comparison due to internal pressure between analytical calculations and 3D ANSYS analysis.	17
Table 4.6 : 3D ANSYS stress analysis results due to internal pressure.	18
Table 4.7 : Percentage differences between 3D and 2D internal pressure ANSYS analysis compared to analytical results.	19
Table 4.8 : Thermal analysis results.....	23
Table 4.9 : Thermal analysis comparison between theoretical calculations and 3D ANSYS simulation.....	24
Table 4.10 : Stress results of 3D ANSYS analysis modeling.	25
Table 4.11 : Percentage differences of von Mises stress between 3D thermal ANSYS analysis and thermal analytical results.	26
Table 4.12 : Combination of thermal and internal pressure stress analysis results on SMR tube.	28
Table 4.13 : Comparison of von Mises stress of theoretical and 3D ANSYS analysis on combination of thermal and internal pressure acting in the SMR tube using N5 parameters.	29
Table 4.14 : 3D ANSYS analysis due to thermal and internal pressure results.....	30
Table 4.15 : Percentage difference of von Mises stress between 3D thermal and internal pressure ANSYS analysis with analytical results.	31

CHAPTER 1

INTRODUCTION

1.1 Background of Study

A steam-methane reformer(SMR) is a device used in steam reforming or auto thermal reforming, and it is a type of chemical synthesis which can produce pure hydrogen gas from natural gas using a catalyst. Steam-methane reforming is commonly used on natural gas with the later being an important source of hydrogen in refineries. There are two natural gas reformer technologies; auto thermal reforming and steam methane reforming. Both methods work by exposing natural gas to a catalyst (usually nickel) at high temperature and pressure.

Steam reforming sometimes referred to as steam methane reforming uses an external source of hot gas to heat tubes in which a catalytic reaction takes place that converts steam and lighter hydrocarbons such as natural gas (methane) or refinery feedstock into hydrogen and carbon monoxide (syngas). Syngas reacts further to produce more hydrogen and carbon dioxide in the reactor. The carbon oxides are removed before use by means of pressure swing adsorption (PSA) with molecular sieves for the final purification. The PSA works by absorbing all impurities from the syngas stream to leave a pure hydrogen gas[1].

1.2 Problem Statement

In a common methanol production process, there are four process stages which were gas preparation, SMR, compression and synthesis, and distillation. This basic SMR process is supported by a process furnace, which provides heat to raise the gas temperature for the endothermic pretreatment and reforming processes. The furnace also provides heat to produce steam, which is used as a reagent in both reforming and gas conversion. In this project, we will fully focus on steam-methane reforming process, and the steam methane reformer tubes. SMR contains hundreds of long vertical tubes operating at high temperature. Creep failure usually occurs to these tubes, where creep is a failure when a material is subjected to stress at high temperature.

SMR operates in a high temperature environment. A SMR contain individuals of vertical SMR tube which is typically fabricated from creep resistant austenitic stainless steel and the estimation of the price of a 12.5m long tube exceeds USD7000. The tube is expected to last 100,000 hours or 11.4 years but in many instances some of these tubes fail prematurely. Since the material cost is a large investment, thorough analysis is needed to predict possible failure to the steam reformer tube in order to save operation and downtime cost. The predictions of failure in SMR tubes require a better determination of stresses due to internal pressure and temperature distribution acted on the tube.

1.3 Objective and Scope of Study

The objective of this project is to determine the stresses present in SMR tube using finite element analysis method. It is anticipated that a better stress determination can improve the failure prediction of SMR tube in order to reduce the cost of economic losses and potential failure. Figure 1.1 shows a general view of SMR tubes.

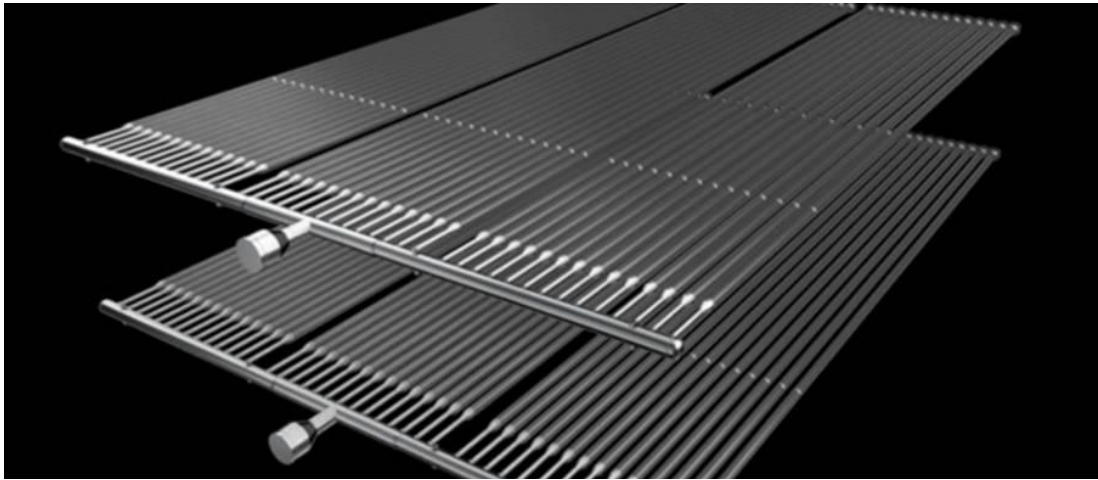


Figure 1.1: General view of SMR tubes

Stress analysis will be conducted using ANSYS by applying pressure on the internal wall and temperature distribution on the steam-methane reformer tube. The analytical and finite element analysis result will then be compared.

The SMR tube to be studied is Schmidt-Clemens Centralloy® CA4852-Micro centrifugally cast austenitic stainless steel[2]. The physical properties and mechanical properties of the material are as follows:

Density = 8.0g/cm^3

Thermal Conductivity = 27.3 W/mK

Poisson's ratio = 0.3

Thermal Expansion = $18.5 \times 10^{-6} / \text{K}$

Young's Modulus of Elasticity = 95 GPa

Gravitational Acceleration = 9.81 m/s^2

CHAPTER 2

LITERATURE REVIEW

2.1 Steam-Methane Reforming (SMR) Process

In plants producing methanol, there were basically four main process; feed gas preparation, steam-methane reforming, compression and synthesis, and distillation. The reformer is probably the most expensive component and the main energy user in methanol plant. Thus this project is mainly focusing on the steam-methane reforming process since it is one of the most important components in methanol plant. In steam-methane reforming process, basically the methane that being feed into the tubes at internal pressure approximately 2MPa will react with each other in the presence of nickel oxide at high temperature to produce carbon monoxide (CO), carbon dioxide (CO₂), and hydrogen (H₂) [1]. This is a highly endothermic reaction which is supported by heat from the reformer furnace. Figure 2.1 shows schematic process of Steam Methane Reformer [3].

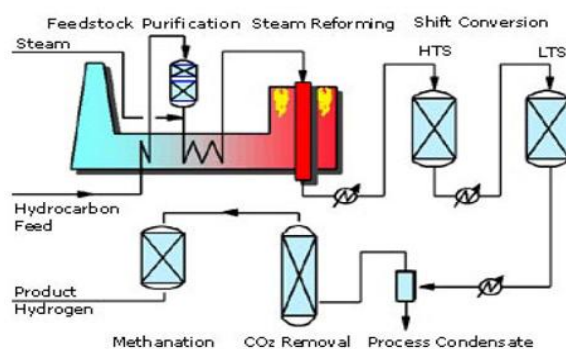
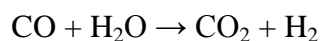
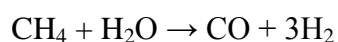


Figure 2.1 : Schematic process of Steam Methane Reformer[3].

Figure 2.2 shows the SMR in operation[4] and Figure 2.3 shows the inside view of the SMR[5].



Figure 2.2 : SMR in operation[4].

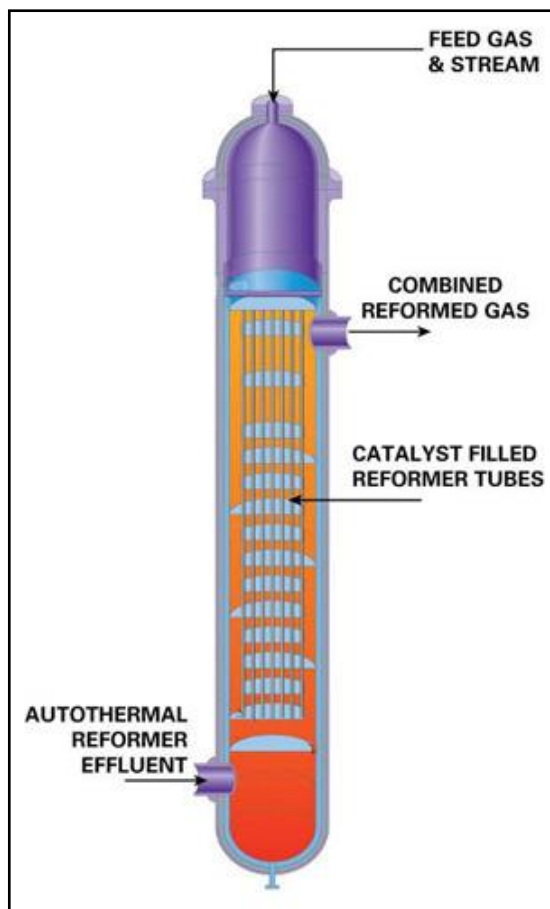


Figure 2.3 : Inside view of the SMR[5].

2.2 Analytical Equations

Basically there were four analytical equations employed in this project. They were stresses due to internal pressure (Lame's equation), thermal stresses calculation, stresses due to tube weight and calculation of the effective stresses. The SMR tube is considered as a thick wall cylinder. As a result of pressure and temperature acting inside the tube, hoop, longitudinal and axial stresses were developed. Effective stress can also be known as von Mises stress.

Stress due to Internal Pressure (Lame's Equation) [6]

$$\text{Hoop Stress: } \sigma_{hp} = \frac{pr_i^2}{r_o^2 - r_i^2} \left(1 + \frac{r_o^2}{r^2} \right) \quad (1a)$$

$$\text{Radial Stress: } \sigma_{rp} = \frac{pr_i^2}{r_o^2 - r_i^2} \left(1 - \frac{r_o^2}{r^2} \right) \quad (1b)$$

$$\text{Axial Stress: } \sigma_{ap} = \frac{pr_i^2}{r_o^2 - r_i^2} \quad (1c)$$

where: p = Internal pressure

r = Radius of internal tube wall

t = Thickness of tube wall

Thermal Stress [7]

$$\text{Hoop Stress= } \sigma_{hT} = \frac{\alpha E (T_i - T_o)}{2(1-\nu)} \left[\frac{1 - \ln\left(\frac{r_o}{r}\right)}{\ln\left(\frac{r_o}{r_i}\right)} - \frac{\left(\frac{r_o}{r}\right)^2 + 1}{\left(\frac{r_o}{r}\right)^2 - 1} \right] \quad (2a)$$

$$\text{Radial Stress= } \sigma_{rT} = \frac{\alpha E (T_i - T_o)}{2(1-\nu)} \left[\frac{-\ln\left(\frac{r_o}{r}\right)}{\ln\left(\frac{r_o}{r_i}\right)} + \frac{\left(\frac{r_o}{r}\right)^2 - 1}{\left(\frac{r_o}{r}\right)^2 - 1} \right] \quad (2b)$$

$$\text{Axial Stress= } \sigma_{aT} = \frac{\alpha E (T_i - T_o)}{2(1-\nu)} \left[\frac{1 - 2\ln\left(\frac{r_o}{r}\right)}{\ln\left(\frac{r_o}{r_i}\right)} - \frac{2}{\left(\frac{r_o}{r}\right)^2 - 1} \right] \quad (2c)$$

where: T_i = Internal temperature
 T_o = External temperature
 r = radial distance to point of interest
(Other variables as defined earlier)

Stress due to Tube Weight

Seventy five percent of tube weight is supported by the tube hangar. The axial stress due to tube weight is:

$$\text{Axial stress: } \sigma_{aW} = 0.25 \times \frac{W}{A} = 0.25 \times \frac{\rho g A l}{A} = 0.25 \times \rho g l \quad (3a)$$

$$\text{Axial stress per length of tube} = \frac{\sigma_{aW}}{l} = -19.62 \times 10^{-3} \text{ MPa/m} \quad (3b)$$

where: W = weight of tube

A = Cross sectional area of tube

ρ = Density of SMR tube = 8000kg/m³ (Schmidt + Clemens, 2001)

g = gravitational acceleration = 9.81m/s²

l = vertical distance from top flange to point of interest.

Negative sign indicates compressive stress.

Effective Stress (von Mises stress) [8]

$$\sigma_v = \sqrt{\frac{(\sigma_1 - \sigma_2)^2 + (\sigma_2 - \sigma_3)^2 + (\sigma_1 - \sigma_3)^2}{2}} \quad (4)$$

where: Hoop Stress = $\sigma_1 = \sigma_{hT} + \sigma_{hP}$

Radial Stress = $\sigma_2 = \sigma_{rT} + \sigma_{rP}$

Axial Stress = $\sigma_3 = \sigma_{aT} + \sigma_{aP} + \sigma_{aW}$

CHAPTER 3

METHODOLOGY

3.1 Finite Element Analysis

Finite element analysis was used to determine possible failure in a material by demonstrating possible virtual load simulation. In this project, analysis on the effect of pressure and temperature on steam-methane reformer tube was done. The tool used in this project was ANSYS Multiphysics.

Basically there were three analyses done on the SMR tube which were:

- a) Stress analysis on SMR tube due to internal pressure.
- b) Stress analysis on SMR tube due to temperature distribution.
- c) Stress analysis on SMR tube due to internal pressure and temperature distribution.

There were three major phases in finite element analysis method which were:

- a) Pre-processing
- b) Solution
- c) Post-processing

In order to be proficient in ANSYS, the following tasks were embarked upon, as shown in the schematic of Figure 3.1.

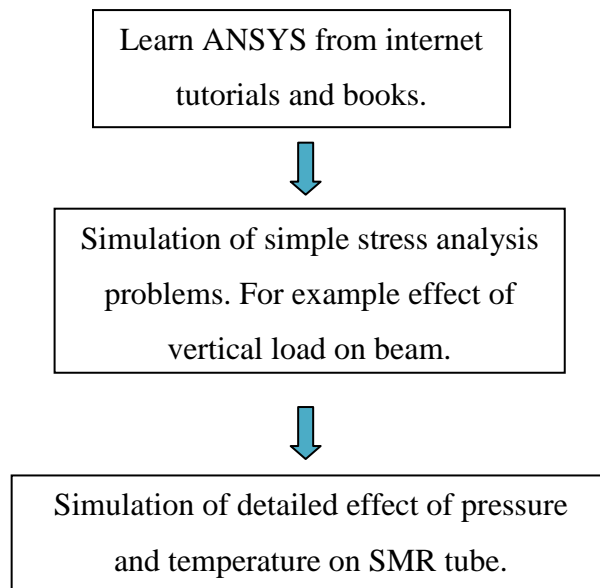


Figure 3.1 : ANSYS learning flowchart.

3.2 SMR ANSYS Workflow

The general workflow used in the ANSYS to study on SMR tubes are as follows:

1. Properties of the SMR tube were defined in the material model behavior box.

Figure 3.2 shows material model behavior box.

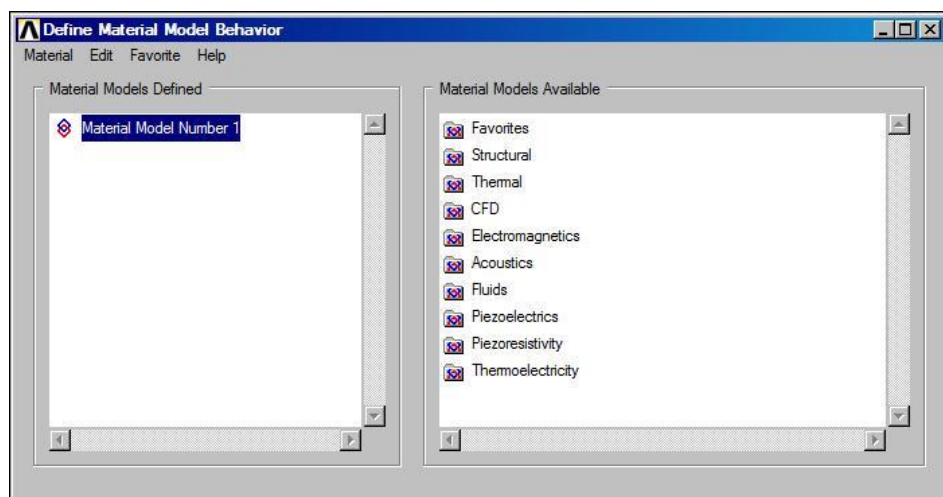


Figure 3.2 : Material model behavior box.

2. The model of the SMR tube was created.
3. Boundary conditions and pressure distribution were applied to the model as in figure 3.3. As you can see, the red arrow shows pressure applied at the tube wall. Noticed the top part of the tube was constrained in y-direction.

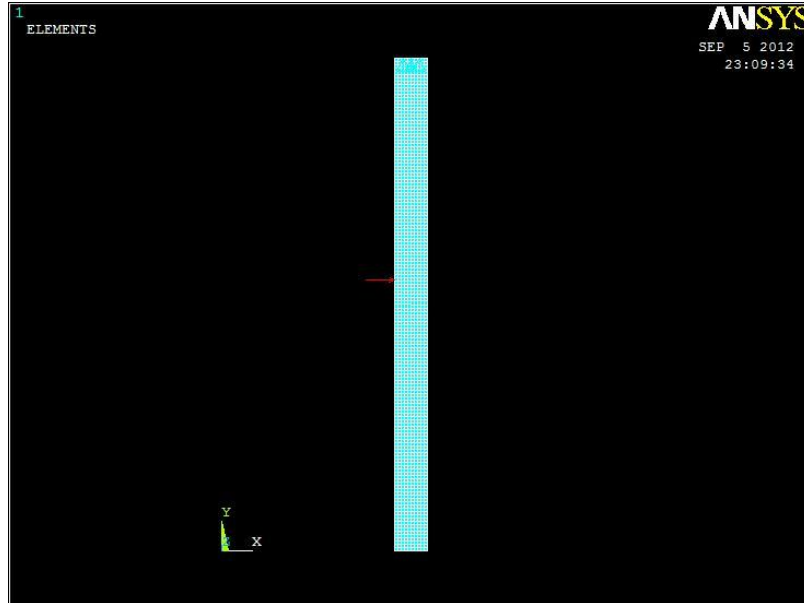


Figure 3.3 : Boundary condition and pressure applied at SMR tube wall.

4. The simulation of SMR tube was solved.
5. Stresses developed in the SMR tube were analyzed in the post-processing. Figure 3.4 shows stress occurred at the tube after the problem was solved.
6. Simulation of thermal stress was basically the same with pressure analysis. Temperature distribution was added at the inner and the outer wall of the tube.

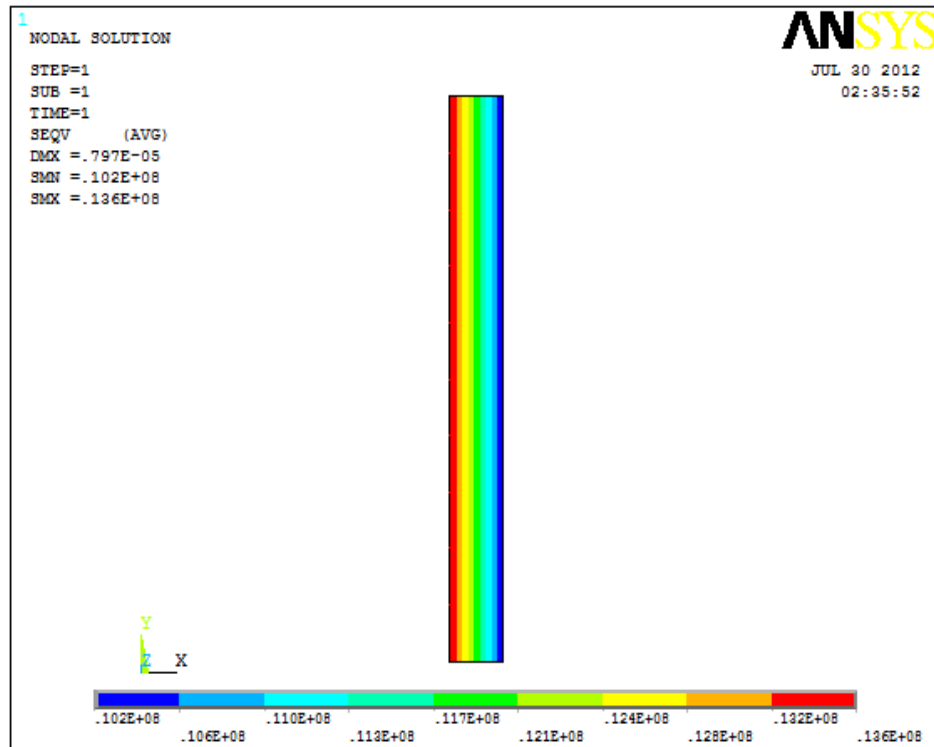


Figure 3.4 : Stress stress occurred at the tube after the problem was solved.

3.3 Gantt Chart

During the first 9 weeks of the Final Year Project 2, project activities included literature search of resources and information about Steam-Methane Reformer tubes. In addition ANSYS stress analyses of SMR tubes were also carried out during this period. Work during weeks 8 to 10 consisted primarily of preparations of progress report. Pre-SEDEX or poster presentation was held during weeks 11 and 12. Finally, draft report, final report and VIVA presentation were done in weeks 13, 14 and 15.

The Gantt chart for this Final Year Project 2 is shown in Figure 3.5.

	week 1	week 2	week 3	week 4	week 5	week 6	week 7	week 8	week 9	week 10	week 11	week 12	week 13	week 14	week 15
Find resources															
ANSYS tasks: <ul style="list-style-type: none"> • define properties • modeling • set boundary conditions • simulate • analysis of results 															
Progress Report															
Pre-SEDEX															
Draft Report															
Final Report															
VIVA															

Figure 3.5: Gantt Chart for Final Year Project 2.

CHAPTER 4

RESULTS AND DISCUSSION

4.1 Parameters of Stress Analysis of Steam-Methane Reformer Tubes

Table 4.1 shows the input parameters used in SMR ANSYS analysis. The data was obtained from an actual SMR plant.

Table 4.1: Input parameters for finite element analysis.

Sample	Distance from top flange, m	Pressure, MPa	Temperature, K
N1-I	2.5	2.16	1048
N1-O			1121
N2-I	5.0	2.07	1097
N2-O			1151
N3-I	7.5	1.99	1119
N3-O			1151
N4-I	10.0	1.91	1141
N4-O			1159
N5-I	12.5	1.82	1151
N5-O			1161

(Note: Samples N1 through N5 represents locations at 2.5m intervals starting at 2.5m to 12.5m from the top inlet flange. I and O represent ‘inner wall’ and ‘outer wall’ locations respectively).

The material properties of the tube are as shown as below:

Density = 8000kg/m³

Thermal Conductivity = 14.6 W/mK

Poisson's ratio = 0.3

Young's Modulus = 105 GPa

Mean coefficient of linear thermal expansion= $1.85 \times 10^{-5}/K$

Gravitational acceleration = 9.81m/s²

4.2 Analysis of Internal Pressure on SMR Tube Wall

Analytical Results of Internal Pressure Analysis

The results of analytical calculations of stresses due to internal pressure of the tube are shown in Table 4.2

Table 4.2 : Analytical results of internal pressure analysis.

Sample ID	Pressure (MPa)	r (mm)	Hoop Stress, σ_h (MPa)	Radial Stress, σ_r (MPa)	Axial Stress, σ_a (MPa)	von Mises stress, σ_o (MPa)
N1-I	2.16	52.5	12.51	-2.16	5.18	12.71
N1-mid		57.5	11.29	-0.94	5.18	10.59
N1-O		62.5	10.35	0.00	5.18	8.97
N2-I	2.07	52.5	11.99	-2.07	4.96	12.18
N2-mid		57.5	10.82	-0.90	4.96	10.15
N2-O		62.5	9.92	0.00	4.96	8.59
N3-I	1.99	52.5	11.53	-1.99	4.77	11.71
N3-mid		57.5	10.40	-0.87	4.77	9.76
N3-O		62.5	9.54	0.00	4.77	8.26
N4-I	1.91	52.5	11.07	-1.91	4.58	11.24
N4-mid		57.5	9.99	-0.83	4.58	9.37
N4-O		62.5	9.16	0.00	4.58	7.93
N5-I	1.82	52.5	10.54	-1.82	4.36	10.71
N5-mid		57.5	9.52	-0.79	4.36	8.93
N5-O		62.5	8.72	0.00	4.36	7.56

Figure 4.1 shows the view of von Mises stress on 2D axisymmetric's internal pressure simulation of SMR tube. Table 4.3 shows the comparison between von Mises stress of analytical and ANSYS analysis on internal pressure acting in the SMR tube using N1 parameters.

Table 4.3 : Stress comparison due to internal pressure between analytical calculations and 2D ANSYS analysis.

Tube Radial Position,mm	Calculated Stress,MPa	Stress from ANSYS,MPa	% difference
52.5 – I	12.7	13.6	-6.56
57.5 – Mid	10.6	11.7	-9.45
62.5 – O	8.97	10.2	-12.09

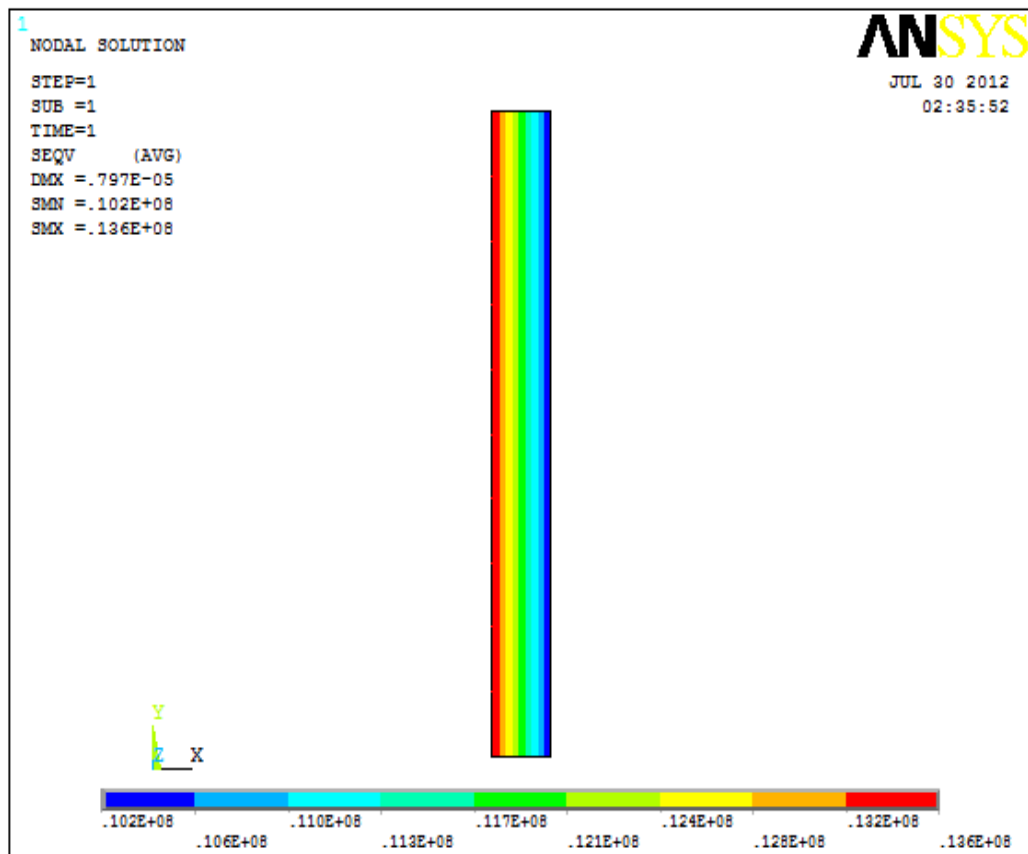


Figure 4.1 : von Mises stress of 2D axisymmetric's internal pressure simulation of SMR tube for N1 parameters.

2D ANSYS Stress Analysis Result due to Internal Pressure

The results of analytical calculations of stresses due to internal pressure of the tube are shown in Table 4.4.

Table 4.4 : Internal pressure 2D ANSYS analysis results.

Sample ID	Pressure (MPa)	r (mm)	Hoop Stress, σ_h (MPa)	Radial Stress, σ_r (MPa)	Axial Stress, σ_a (MPa)	von Mises stress, σ_o (MPa)
N1-I	2.16	52.5	12.40	-2.06	0.00	13.60
N1-mid		57.5	11.20	-1.14	0.04	11.70
N1-O		62.5	10.30	0	0.09	10.20
N2-I	2.07	52.5	11.90	-1.97	0.00	13.00
N2-mid		57.5	10.80	-1.10	0.04	11.20
N2-O		62.5	9.84	0	0.08	9.80
N3-I	1.99	52.5	11.40	-1.90	0.00	12.50
N3-mid		57.5	10.30	-1.05	0.04	10.80
N3-O		62.5	9.46	0	0.08	9.42
N4-I	1.91	52.5	11.00	0.08	0.00	12.00
N4-mid		57.5	9.92	0.03	-1.01	10.40
N4-O		62.5	9.08	0	-1.82	9.04
N5-I	1.82	52.5	10.50	0.07	0.00	11.40
N5-mid		57.5	9.45	0.03	-0.96	9.86
N5-O		62.5	8.65	0.00	-1.73	8.62

Figure 4.2 below shows the view of von Mises stress on 3D ANSYS modelling of internal pressure simulation of SMR tube. Table 4.5 shows the comparison of von Mises stress of analytical and 3D ANSYS analysis on internal pressure acting in the SMR tube using N1 data.

Table 4.5 : Effective stress comparison due to internal pressure between analytical calculations and 3D ANSYS analysis.

Tube Radial Position,mm	Calculated Stress,MPa	Stress from ANSYS,MPa	% difference
52.5 – I	12.7	13.8	-7.97
57.5 – Mid	10.6	11.5	-7.82
62.5 – O	8.97	10.37	-13.5

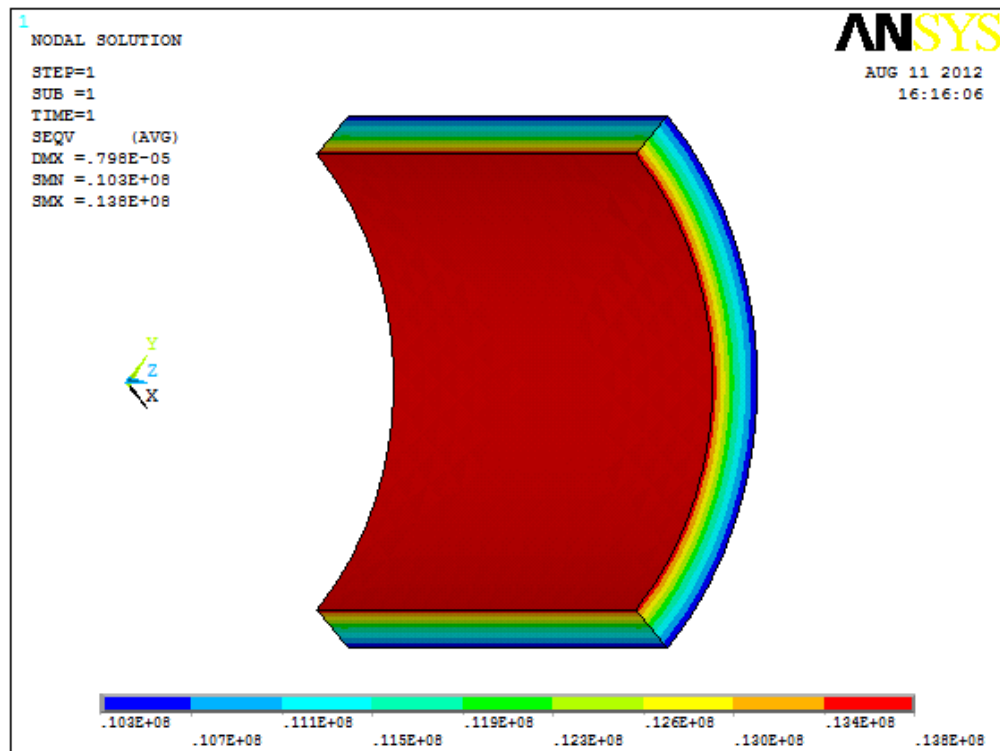


Figure 4.2 : von Mises stress of 3D ANSYS simulation due to internal pressure of SMR tube for N1 parameters.

3D ANSYS Stress Analysis Result due Internal Pressure

The results of 3D ANSYS stress analysis due to internal pressure of the tube are shown in Table 4.6.

Table 4.6 : 3D ANSYS stress analysis results due to internal pressure.

Sample ID	Pressure (MPa)	r (mm)	Hoop Stress, σ_h (MPa)	Radial Stress, σ_r (MPa)	Axial Stress, σ_a (MPa)	von Mises stress, σ_o (MPa)
N1-I	2.16	52.5	12.6	-2.23	0.009	13.80
N1-mid		57.5	11.4	-1.21	0.009	11.50
N1-O		62.5	10.30	0.06	0.009	10.37
N2-I	2.07	52.5	12.1	-2.14	0.009	13.20
N2-mid		57.5	10.9	-1.16	0.009	11.00
N2-O		62.5	9.91	0.05	0.009	9.90
N3-I	1.99	52.5	11.6	-2.06	0.009	12.70
N3-mid		57.5	10.50	-1.12	0.009	10.60
N3-O		62.5	9.53	0.05	0.009	9.52
N4-I	1.91	52.5	11.2	-1.97	0.008	12.20
N4-mid		57.5	10.0	-1.07	0.008	10.20
N4-O		62.5	9.14	0.05	0.008	9.14
N5-I	1.82	52.5	10.6	-1.88	0.008	11.60
N5-mid		57.5	9.57	-1.02	0.008	9.68
N5-O		62.5	8.71	0.05	0.008	8.71

Table 4.7 shows the percentage differences between 3D and 2D internal pressure ANSYS analysis compared to analytical results.

Table 4.7 : Percentage differences between 3D and 2D internal pressure ANSYS analysis compared to analytical results.

Sample ID	Analytical	3D ANSYS	Percentage Difference, %	2D ANSYS	Percentage Difference, %
N1-I	12.71	13.80	7.90	13.60	6.54
N1-mid	10.59	11.50	7.91	11.70	9.49
N1-O	8.97	10.37	13.50	10.20	12.06
N2-I	12.18	13.20	7.73	13.00	6.31
N2-mid	10.15	11.00	7.73	11.20	9.37
N2-O	8.59	9.90	13.23	9.80	12.35
N3-I	11.71	12.70	7.80	12.50	6.32
N3-mid	9.76	10.60	7.92	10.80	9.63
N3-O	8.26	9.52	13.24	9.42	12.31
N4-I	11.24	12.20	7.87	12.00	6.33
N4-mid	9.37	10.20	8.14	10.40	9.90
N4-O	7.93	9.14	13.24	9.04	12.28
N5-I	10.71	11.60	7.67	11.40	6.05
N5-mid	8.93	9.68	7.75	9.86	9.43
N5-O	7.56	8.71	13.20	8.62	12.30

Figure 4.3 shows comparison of line trend between 2D ANSYS axisymmetric, 3D ANSYS modeling and analytical calculation of effective stress due to internal pressure for sample N1.

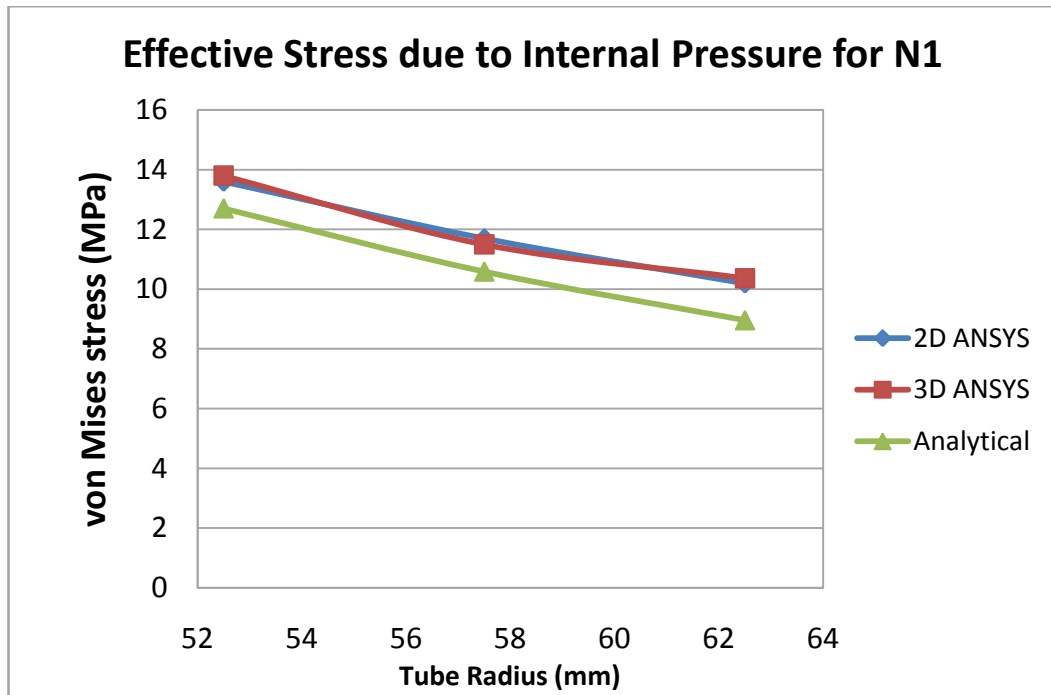


Figure 4.3 : Comparison of line trend between 2D ANSYS, 3D ANSYS and analytical calculation of effective stress due to internal pressure for N1.

It can be seen that the effective stress is decreasing from inner to the outer tube radius. The percentage difference of resultant effective stress between analytical, 2D analysis and 3D analysis is in 10% range. Results calculated using data for N2, N3, N4 and N5 follow the same line trend with line N1.

Figure 4.4 and 4.5 show analytical and 2D ANSYS axisymmetric analysis of effective stress due to internal pressure versus tube radius.

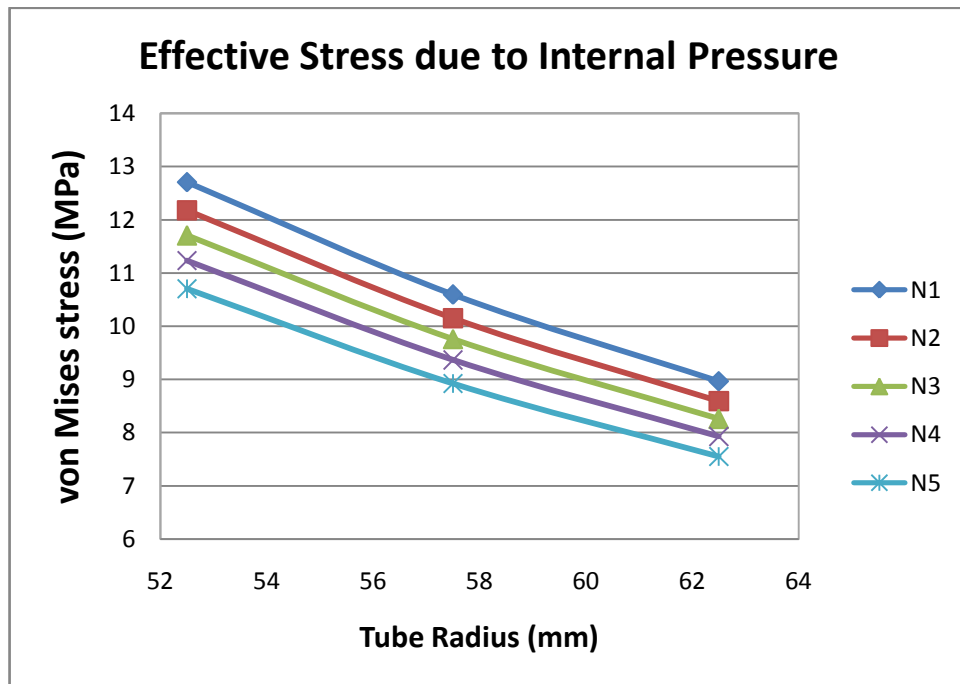


Figure 4.4 : Analytical effective stress due to internal pressure versus tube radius.

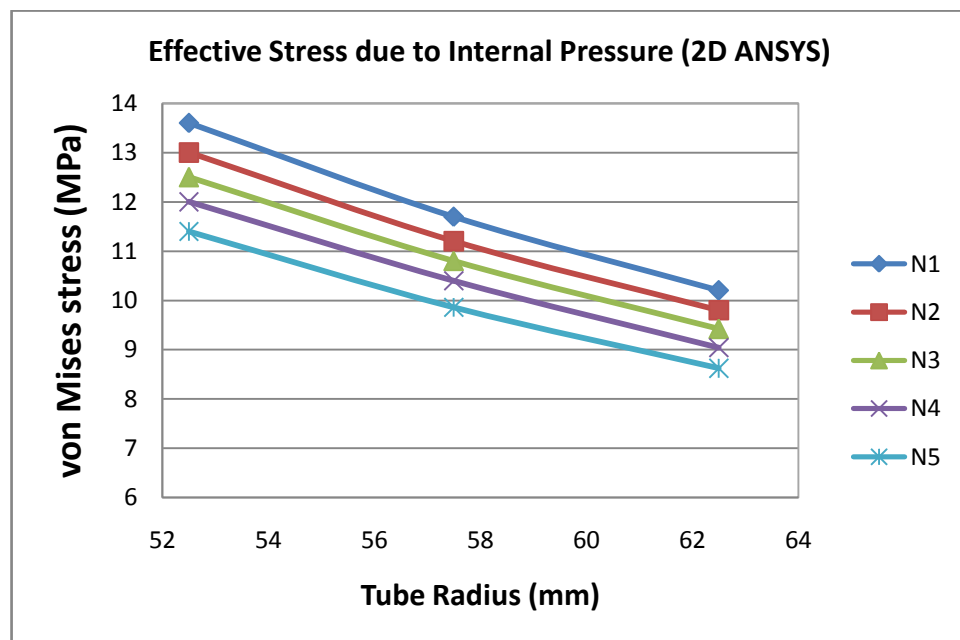


Figure 4.5 : Effective stress of 2D ANSYS analysis due to internal pressure versus tube radius.

Figure 4.6 and 4.7 show 3D internal pressure ANSYS analysis and overlapping of analytical, 2D and 3D analysis of effective stress due to internal pressure versus tube radius.

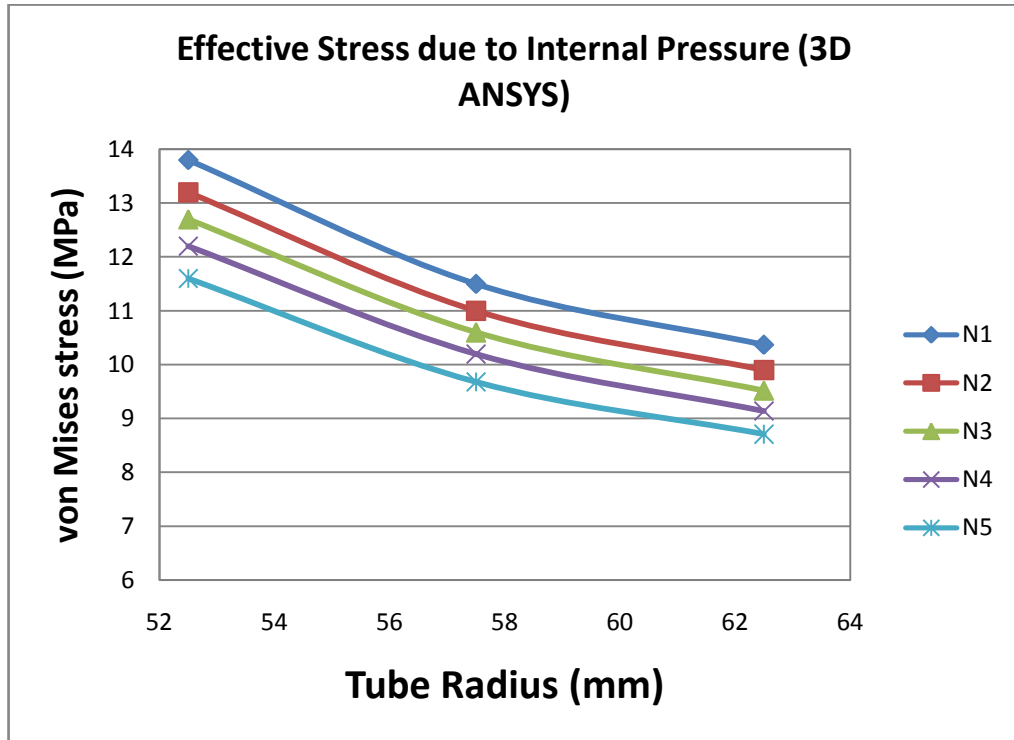


Figure 4.6 : Effective stress of 3D ANSYS analysis due to internal pressure versus tube radius.

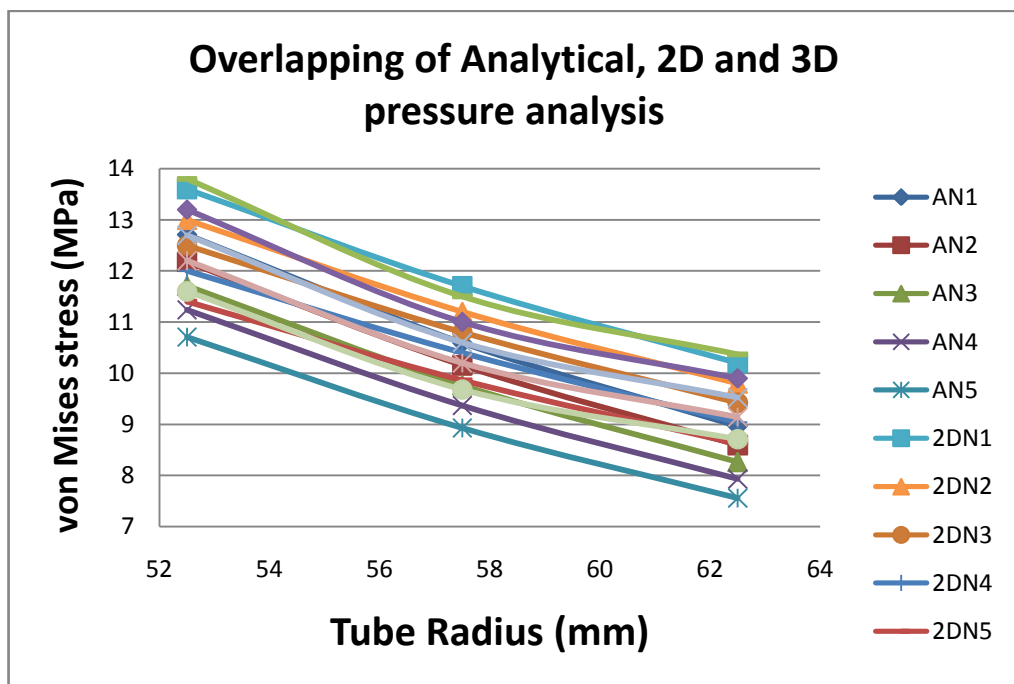


Figure 4.7 : Overlapping of analytical, 2D and 3D pressure analysis.

4.3 Analysis of Temperature Distribution on SMR Tube Wall

Analytical Stress Results of Thermal Analysis

The results of analytical calculations of stresses due to temperature profile of the tube are shown in Table 4.8

Table 4.8 : Thermal analysis results.

Sample ID	Pressure (MPa)	r (mm)	Hoop Stress, σ_h (MPa)	Radial Stress, σ_r (MPa)	Axial Stress, σ_a (MPa)	von Mises stress, σ_o (MPa)
N1-I	2.16	52.5	96.96	0	96.96	96.96
N1-mid		57.5	-2.64	3.97	1.33	5.76
N1-O		62.5	-86.33	0	-86.33	86.33
N2-I	2.07	52.5	71.72	0	71.72	71.72
N2-mid		57.5	-1.95	2.93	0.98	4.26
N2-O		62.5	-63.86	0	-63.86	63.86
N3-I	1.99	52.5	42.50	0	42.50	42.50
N3-mid		57.5	-1.16	1.74	0.58	2.53
N3-O		62.5	-37.84	0	-37.84	37.84
N4-I	1.91	52.5	23.91	0	23.91	23.91
N4-mid		57.5	-0.65	0.98	0.33	1.42
N4-O		62.5	-21.29	0	-21.29	21.29
N5-I	1.82	52.5	13.28	0	13.28	13.28
N5-mid		57.5	-0.36	0.54	0.18	0.79
N5-O		62.5	-11.83	0	-11.83	11.83

Figure 4.8 shows von Mises stress of 3D thermal analysis modelling. Table 4.9 list the comparison of von Mises stress of analytical and ANSYS analysis on temperature acting in the SMR tube using sample N1.

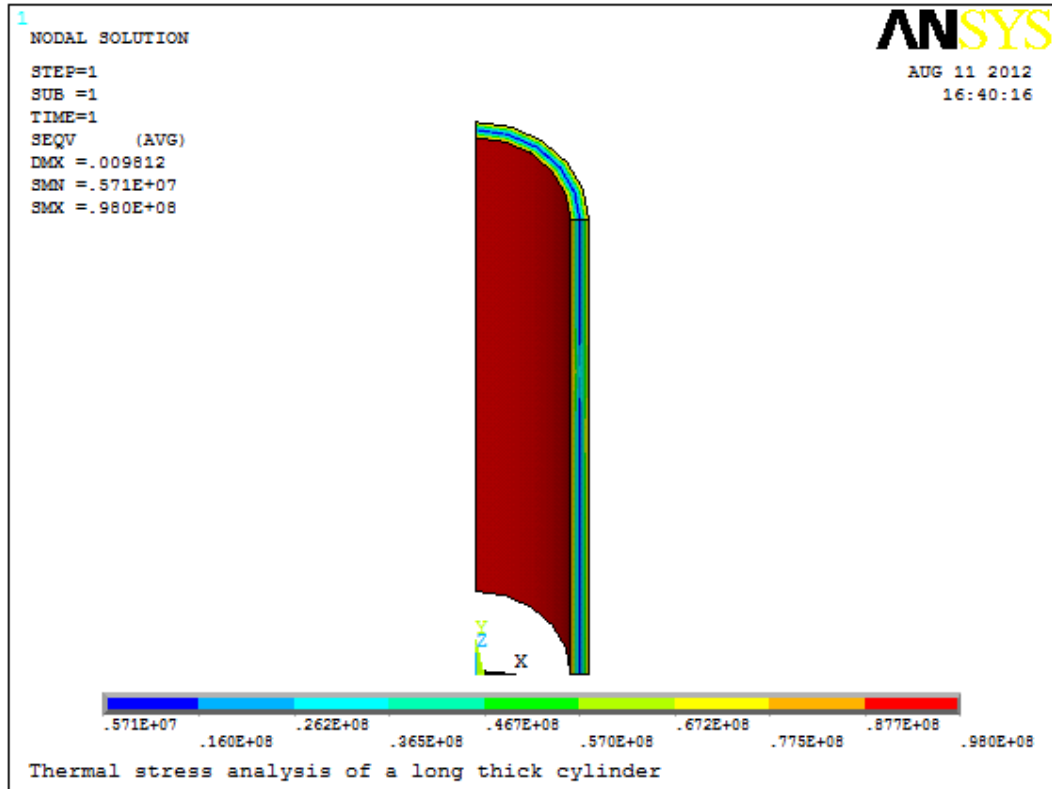


Figure 4.8 : 3D thermal ANSYS analysis modelling for N1 parameters.

Table 4.9 : Thermal analysis comparison between theoretical calculations and 3D ANSYS simulation.

Tube Radial Position,mm	Calculated Stress,MPa	Stress from ANSYS,MPa	% difference
52.5 – I	97	98	-1.07
57.5 – Mid	5.76	5.71	0.89
62.5 – O	86.3	87.7	-1.57

Stress results of 3D ANSYS thermal analysis modeling.

The results of analytical calculations of stresses due to temperature profile of the tube are shown in Table 4.10.

Table 4.10 : Stress results of 3D ANSYS analysis modeling.

Sample ID	Pressure (MPa)	r (mm)	Hoop Stress, σ_h (MPa)	Radial Stress, σ_r (MPa)	Axial Stress, σ_a (MPa)	von Mises stress, σ_o (MPa)
N1-I	2.16	52.5	100.00	1.90	95.80	98.00
N1-mid		57.5	32.60	-19.50	-4.91	5.71
N1-O		62.5	-7.83	-73.10	-85.50	87.70
N2-I	2.07	52.5	74.00	1.41	70.90	72.50
N2-mid		57.5	14.20	-14.40	-3.63	4.22
N2-O		62.5	-5.79	-62.00	-63.20	64.90
N3-I	1.99	52.5	43.90	0.83	42.00	43.00
N3-mid		57.5	14.30	-3.86	-2.15	2.50
N3-O		62.5	-34.30	-36.70	-37.50	38.50
N4-I	1.91	52.5	24.70	0.47	23.60	24.20
N4-mid		57.5	8.05	-2.17	-1.21	1.41
N4-O		62.5	-1.93	-20.70	-21.10	21.60
N5-I	1.82	52.5	13.70	0.26	13.10	13.40
N5-mid		57.5	2.62	-1.21	-0.67	0.78
N5-O		62.5	-1.07	-11.50	-11.70	12.00

Percentage differences of von Mises stress between 3D thermal ANSYS analysis and thermal analytical results are shown in Table 4.11

Table 4.11 : Percentage differences of von Mises stress between 3D thermal ANSYS analysis and thermal analytical results.

Sample ID	Pressure (MPa)	r (mm)	3D ANSYS	Analytical	Percentage Difference, %
N1-I	2.16	52.5	98	96.96	-1.07
N1-mid		57.5	5.71	5.76	0.87
N1-O		62.5	87.7	86.33	-1.59
N2-I	2.07	52.5	72.5	71.72	-1.09
N2-mid		57.5	4.22	4.26	0.94
N2-O		62.5	64.9	63.86	-1.63
N3-I	1.99	52.5	43	42.5	-1.18
N3-mid		57.5	2.5	2.53	1.19
N3-O		62.5	38.5	37.84	-1.74
N4-I	1.91	52.5	24.2	23.91	-1.21
N4-mid		57.5	1.41	1.42	0.70
N4-O		62.5	21.6	21.29	-1.46
N5-I	1.82	52.5	13.4	13.28	-0.90
N5-mid		57.5	0.78	0.79	1.27
N5-O		62.5	12	11.83	-1.44

Figure 4.9 shows comparison of line trend between 3D thermal ANSYS analysis and analytical calculation of effective stress due to temperature for sample N1.

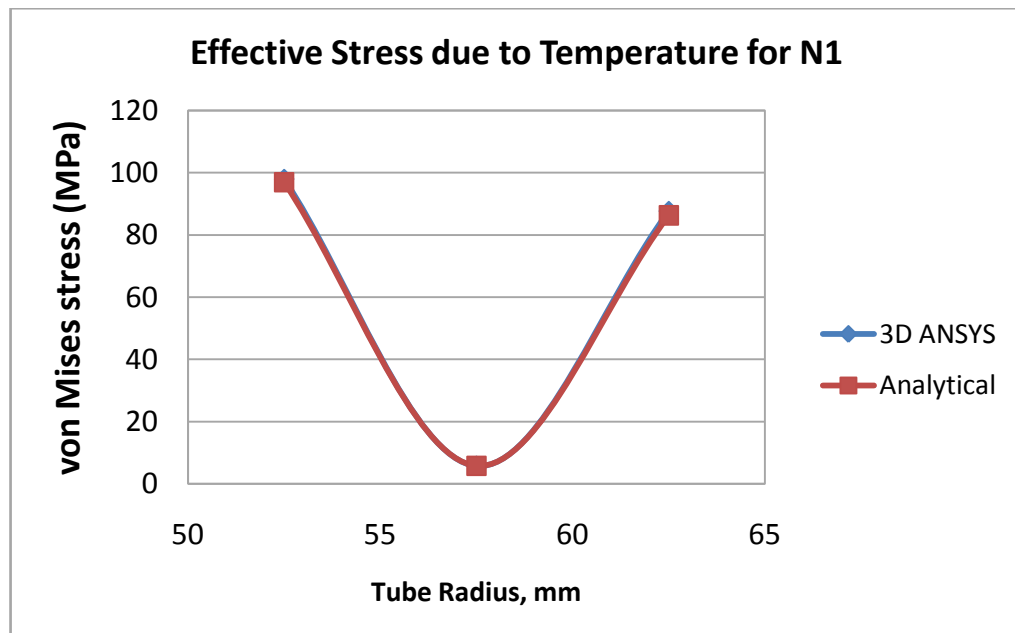


Figure 4.9 : Comparison of line trend between 3D thermal ANSYS analysis and analytical calculation of effective stress due to temperature for sample N1.

It can be seen that the effective stress is decreasing from inner to the center tube wall and then increased back to the outer tube wall. The percentage difference of resultant effective stress between analytical, 3D analysis and analytical analysis is in 10% range. Sample N2, N3, N4 and N5 follow the same line trend with line N1.

Figure 4.10 and 4.11 show theoretical and 3D ANSYS analysis of effective stress due to temperature distribution versus tube radius.

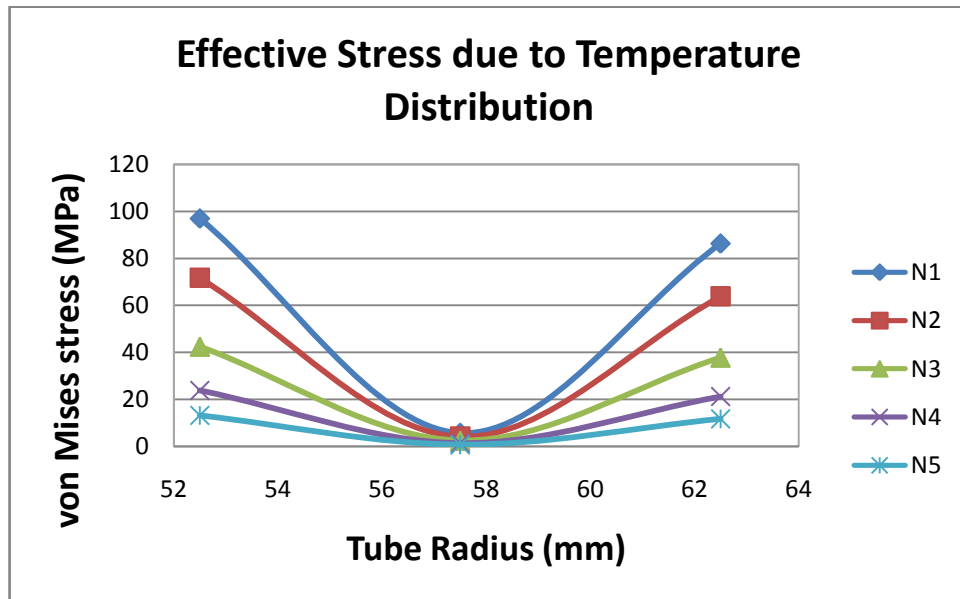


Figure 4.10 : Analytical effective stress due to temperature distribution versus tube radius.

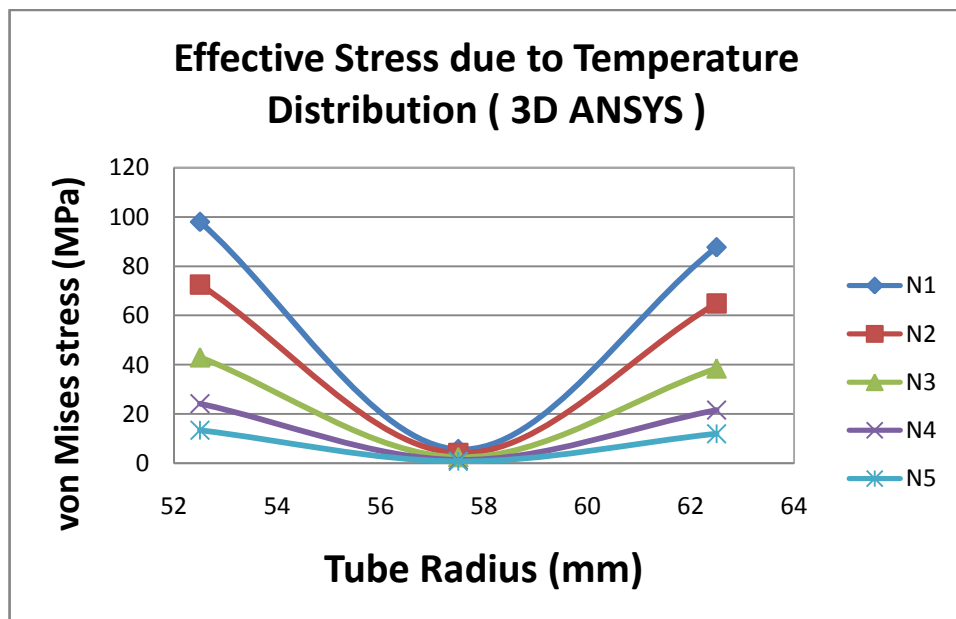


Figure 4.11 : 3D ANSYS analysis effective stress due to temperature distribution versus tube radius.

4.4 Stress Analysis of Temperature Distribution and Internal Pressure on SMR Tube Wall.

The results of analytical calculations of stresses due to thermal and internal pressure of the tube are shown in table 4.12.

Table 4.12 : Combination of thermal and internal pressure stress analysis results on SMR tube.

Sample ID	Pressure (MPa)	r (mm)	Hoop Stress, σ_h (MPa)	Radial Stress, σ_r (MPa)	Axial Stress, σ_a (MPa)	von Mises stress, σ_o (MPa)
N1-I	2.16	52.5	109.47	-2.16	102.08	108.13
N1-mid		57.5	8.65	3.03	6.45	4.91
N1-O		62.5	-75.97	0	-81.20	78.72
N2-I	2.07	52.5	83.71	-2.07	76.58	82.45
N2-mid		57.5	8.87	2.03	5.84	5.93
N2-O		62.5	-53.93	0	-58.99	56.63
N3-I	1.99	52.5	54.03	-1.99	47.12	52.91
N3-mid		57.5	9.25	0.87	5.20	7.25
N3-O		62.5	-28.30	0	-33.22	31.05
N4-I	1.91	52.5	34.97	-1.91	28.29	34.04
N4-mid		57.5	9.34	0.15	4.71	7.96
N4-O		62.5	-12.13	0	-16.90	15.09
N5-I	1.82	52.5	23.83	-1.82	17.40	23.11
N5-mid		57.5	9.15	-0.25	4.30	8.14
N5-O		62.5	-3.10	0	-7.71	6.72

Figure 4.12 below shows 3D thermal and internal analysis modeling of quarter SMR tube. Table 4.13 list the comparison of von Mises stress between theoretical and 3D ANSYS analysis on combination of thermal and internal pressure acting in the SMR tube using parameters N5.

Table 4.13 : Comparison of von Mises stress of theoretical and 3D ANSYS analysis on combination of thermal and internal pressure acting in the SMR tube using N5 parameters.

Tube Radial Position,mm	Calculated Stress,MPa	Stress from ANSYS,MPa	% difference
52.5 – I	23.11	22.80	1.35
57.5 – Mid	8.14	8.80	-8.06
62.5 – O	6.72	7.05	-4.94

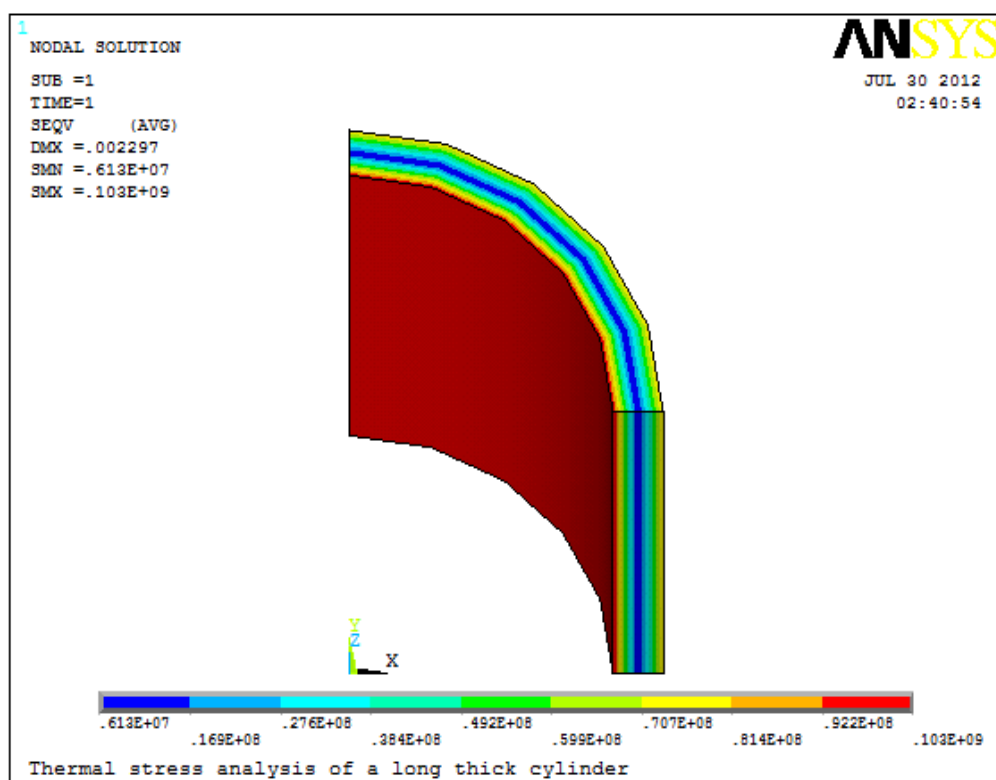


Figure 4.12 : 3D thermal and internal pressure ANSYS analysis modelling of quarter SMR tube.

Stress results of 3D ANSYS thermal and internal pressure analysis modeling.

The results of 3D ANSYS thermal and internal pressure analysis modeling of the tube are shown in Table 4.14

Table 4.14 : 3D ANSYS analysis due to thermal and internal pressure results.

Sample ID	Pressure (MPa)	r (mm)	Hoop Stress, σ_h (MPa)	Radial Stress, σ_r (MPa)	Axial Stress, σ_a (MPa)	von Mises stress, σ_o (MPa)
N1-I	2.16	52.5	112.00	5.84	96.40	107.00
N1-mid		57.5	8.90	-4.53	-1.87	5.82
N1-O		62.5	-20.50	-87.50	-80.50	72.60
N2-I	2.07	52.5	85.40	4.36	71.40	81.70
N2-mid		57.5	7.36	-3.28	-0.27	4.43
N2-O		62.5	-3.79	-64.40	-57.60	55.90
N3-I	1.99	52.5	55.10	2.30	42.30	52.10
N3-mid		57.5	5.69	-2.19	1.56	6.28
N3-O		62.5	-1.37	-38.10	-31.10	31.70
N4-I	1.91	52.5	35.60	-1.53	23.80	33.40
N4-mid		57.5	9.17	-4.02	2.67	6.97
N4-O		62.5	0.37	-21.50	-14.30	15.80
N5-I	1.82	52.5	24.20	-2.35	13.20	22.80
N5-mid		57.5	10.20	-0.99	2.70	8.80
N5-O		62.5	-10.70	-11.90	3.63	7.05

Percentage differences of von Mises stress between 3D thermal and internal pressure ANSYS analysis and analytical results are shown in Table 4.15.

Table 4.15 : Percentage difference of von Mises stress between 3D thermal and internal pressure ANSYS analysis with analytical results.

Sample ID	Pressure (MPa)	r (mm)	3D ANSYS	Analytical	Percentage Difference, %
N1-I	2.16	52.5	107	108.13	1.05
N1-mid		57.5	5.82	4.91	-18.53
N1-O		62.5	72.6	78.72	7.77
N2-I	2.07	52.5	81.7	82.45	0.91
N2-mid		57.5	4.43	5.93	25.30
N2-O		62.5	55.9	56.63	1.29
N3-I	1.99	52.5	52.1	52.91	1.53
N3-mid		57.5	6.28	7.25	13.38
N3-O		62.5	31.7	31.05	-2.09
N4-I	1.91	52.5	33.4	34.04	1.88
N4-mid		57.5	6.97	7.96	12.44
N4-O		62.5	15.8	15.09	-4.71
N5-I	1.82	52.5	22.8	23.11	1.34
N5-mid		57.5	8.8	8.14	-8.11
N5-O		62.5	7.05	6.72	-4.91

Figure 4.13 shows comparison of line trend between 3D ANSYS analysis and analytical calculation of effective stress due to temperature and internal pressure for sample N1.

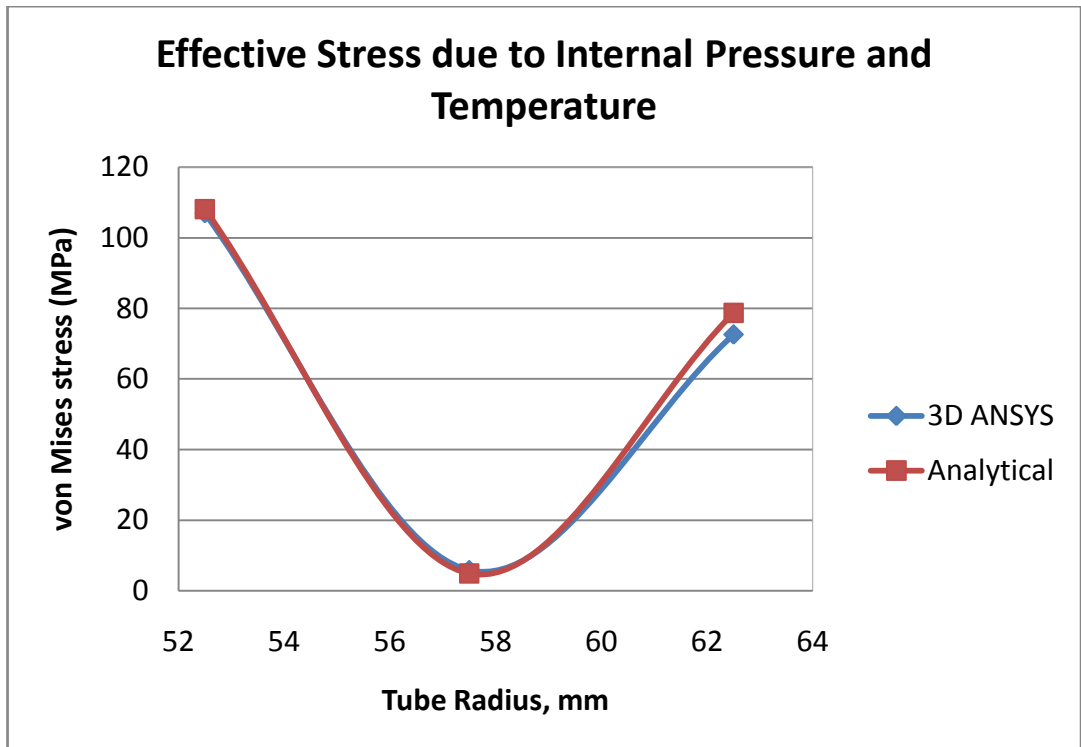


Figure 4.13 : Comparison of line trend between 3D ANSYS analysis and analytical calculation of effective stress due to temperature and internal pressure for sample N1.

It can be seen that the effective stress is decreasing from inner to the center tube wall and then increased back to the outer tube wall. The percentage difference of resultant effective stress between analytical, 3D analysis and analytical analysis is in 10% range. Sample N2, N3, N4 and N5 follow the same line trend with line N1.

Figure 4.14 and 4.15 show theoretical and 3D ANSYS analysis of effective stress due to thermal and internal pressure versus tube radius.

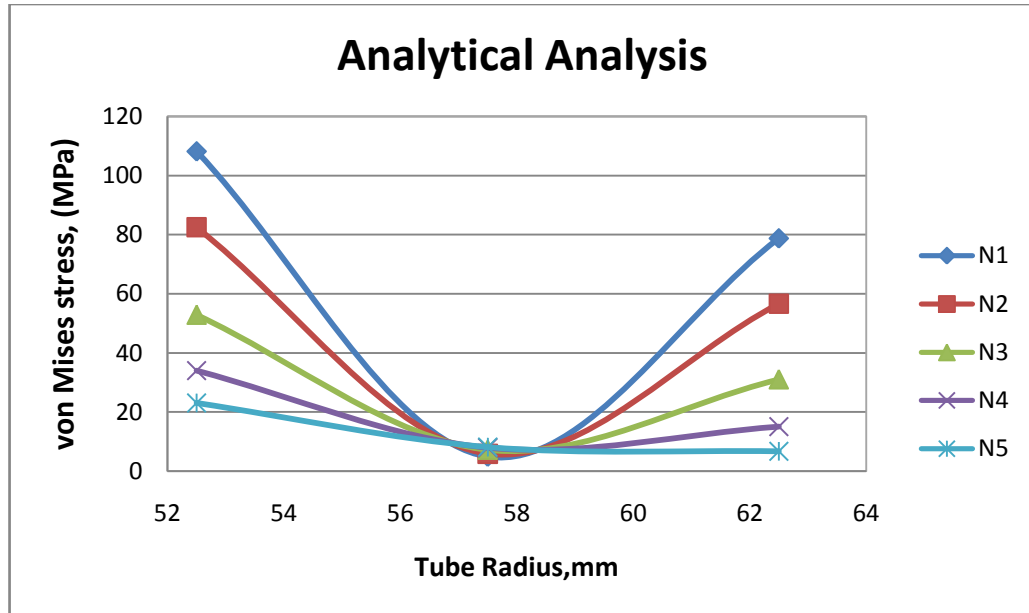


Figure 4.14 : Theoretical effective stress due to temperature and pressure versus tube radius.

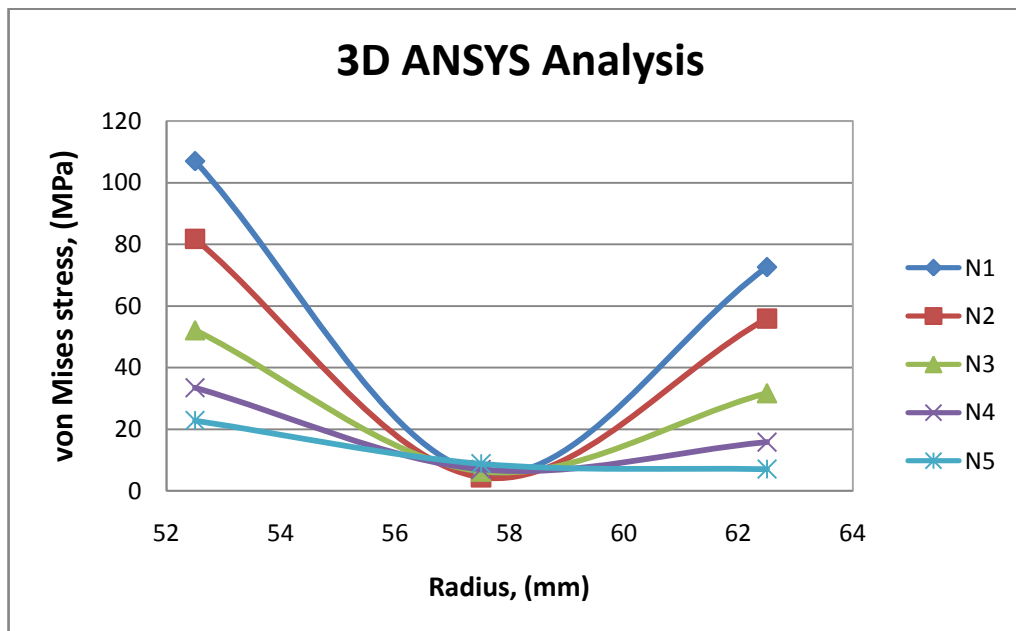


Figure 4.15 : ANSYS analysis effective stress due to temperature and pressure versus tube radius.

CHAPTER 5

CONCLUSION AND RECOMMENDATION

ANSYS Multiphysics software is very useful in determining effective stress that occurs at Steam-Methane Reformer (SMR) tube as it follows the same trends of result as the analytical calculation of effective stress. There were basically few methods in ANSYS for determining stress developed in SMR tube such as 2D axisymmetric and 3D ANSYS modeling. Usually 3D ANSYS analysis is more complex compared to 2D ANSYS analysis.

Boundary condition is a very important segment in ANSYS analysis as it widely influenced the resultant stresses. Slight changes in boundary conditions will lead to different outcomes. Slight difference between analytical and ANSYS analysis results is because finite element method used numerical analysis solutions for each results of its model elements [9]. Besides, the size of the element can also help to increase the accuracy of the result.

One of the major concerns in the operation and maintenance of a reformer is being able to monitor and predict the behavior of the reformer tubes.

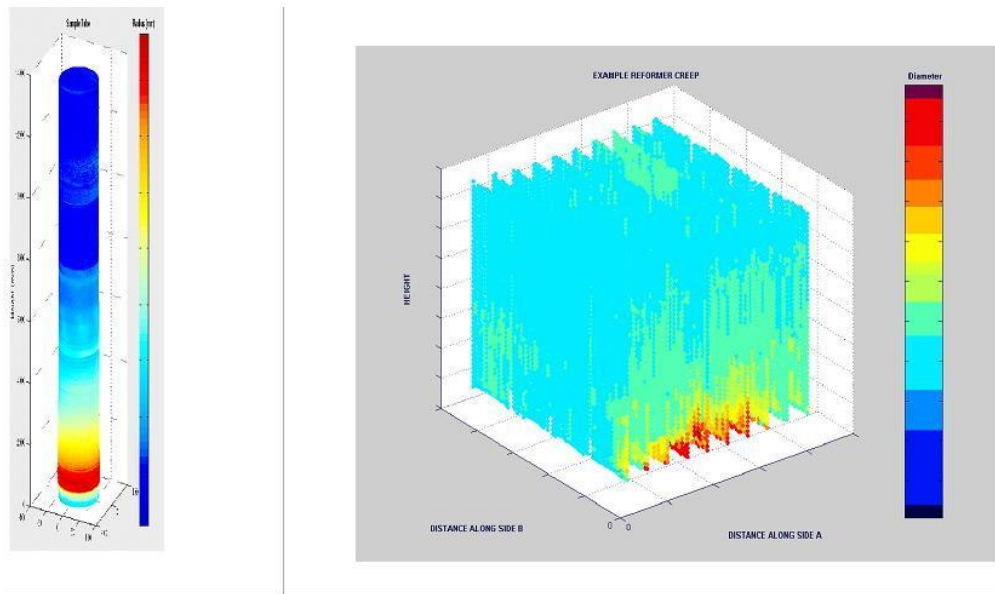


Figure 5.1 : 3D images of creep failure on SMR tube by LOTIS system[9].

Figure 5.1 shows 3D images of creep failure on SMR tube by LOTIS system. LOTIS system is a device used to calculate the percentage expansion of SMR tube during operation. Red area at the near bottom of the tube shows creep failure has occurred. Thus, further failure prediction analysis is needed on the SMR tube before the operation started.

For future work, it would be recommended that other additional variables should be considered in performing the analysis, such as the convection and radiation properties of the material. Heat transfer in the tube probably would occur through convection, conduction and radiation. These variables are very essential in determining the von Mises stress developed along the tube. Stresses developed in tube can then be used in determining the service life of the reformer tube more accurately.

REFERENCE

- [1] John C. Molburg, Richard D. Doctor Hydrogen 2003, Steam-Methane Reforming with CO₂ Capture.
- [2] Schmidt+Clemens Group, Schmidt-Clemens Centralloy® CA4852-Micro Material Data Sheet, 2001, Schmidt+Clemens Group: Lindlar-Kaiserau, Germany.
- [3] Making Hydrogen, 1986, <<http://www.making-hydrogen.com/steam-reforming-hydrogen.html>>
- [4] Schmidt+Clemens Group, 2012, <<http://www.schmidt-clemens.com/branches/sc-spun-casting-petrochemical-ind/components-for-steam-reformer.html>>
- [5] KBR Reforming Exchanger System (KRES™), 1994, <<http://www.kbr.com/Technologies/Proprietary-Equipment/KBR-Reforming-Exchanger-System/>>
- [6] Muvdi, B.B. and McNabb, J.W., Engineering mechanics of materials. 3rd ed. 1991, New York: Springer-Verlag.
- [7] Morozov, E.M. and Fridman, I.B., Thermal stresses and their calculation, in Strength and deformation in nonuniform temperature fields; a collection of scientific papers, Fridman, I.B., Editor. 1964, Consultants Bureau: New York.
- [8] Dowling, N.E., Mechanical Behavior of Materials: Engineering Methods for Deformation, Fracture, and Fatigue. 2nd ed. 1999, Upper Saddle River, NJ: Prentice Hall.
- [9] Steve Roensch, 2005, <http://www.finiteelement.com/newsletter/CourtroomFEA_VolO2.html>